DOI:10.1021/jf103263p

JOURNAL OF AGRICULTURAL AND FOOD CHEMISTRY
ARTICLE

Electrochemical Detection of Amaranth in Food Based on the Enhancement Effect of Carbon Nanotube Film

Peng Wang,[†] Xiaozhong Hu,[†] Qin Cheng,[‡] Xiaoya Zhao,[†] Xiaofang Fu,[†] and Kangbing Wu*,[†,‡]

[†]Technology Center, Hubei Entry-Exit Inspection and Quarantine Bureau, Wuhan 430022, China, and [‡]School of Chemistry and Chemical Engineering, Huazhong University of Science and Technology, Wuhan 430074, China

Amaranth is widely added to food and can cause many adverse health effects when it is excessively consumed. Therefore, the monitoring of amaranth is quite important. Herein, an electrochemical sensor for the sensitive and rapid detection of amaranth was reported using multiwall carbon nanotube (MWNT) as the sensing film. Due to the large surface area and high accumulation efficiency, the MWNT sensor showed a strong enhancement effect on the oxidation of amaranth, and greatly increased the current signal. The detection conditions such as pH value, amount of MWNT, accumulation potential and time were optimized. The linear range is from 40 nM to 0.8 μM, and the limit of detection is 35 nM. Finally, the new sensor was successfully employed to detect amaranth in soft drinks, and the results were tested by high-performance liquid chromatography.

KEYWORDS: Amaranth; rapid detection; electrochemical sensor; carbon nanotube; food analysis

INTRODUCTION

Compared with natural dyes, synthetic dyes have many merits such as high stability to light, oxygen and pH, color uniformity, low microbiological contamination and low production cost. Therefore, synthetic dyes have been widely added into foodstuffs and drinks to make them more attractive and appealing. However, many of them can be pathogenic, particularly when they are excessively consumed (*1*, *2*).

Amaranth as shown in **Figure 1** is a synthetic azo dye, and it is used extensively to give fascinating red color to drinks, syrups and sweets. Studies have shown that amaranth can cause many adverse health effects such as high genotoxicity, cytostaticity and cytotoxicity (*3*). In China, amaranth is permitted and the value of acceptable daily intake (ADI) is between 0 and 0.5 mg kg^{-1} according to the hygienic standards for uses of food additive (GB 2760-1996). Therefore, the detection of amaranth in food is quite important for controlling the food quality and guaranteeing the consumers' safety. Until now, several methods have been applied for the detection of amaranth, such as spectrophotometry (*4*) and high-performance liquid chromatography (*5*, *6*). Amaranth was also detected using electrochemical methods since its −N═N− group can be reduced at the electrode surface (*7*−*12*). For example, a ratio derivative voltammetry (*13*) and a square-wave adsorptive stripping voltammetry (*14*) using hanging mercury drop electrode (HMDE) were reported for the detection of amaranth. However, these methods have some intrinsic drawbacks. First, a toxic mercury electrode is used, leading to environmental pollution and adverse health effects. Second, soluble oxygen heavily influences the reduction signal of amaranth, and must be totally removed from the solution before detection.

Carbon nanotubes (CNTs), including single-wall carbon nanotube (SWNT) and multiwall carbon nanotube (MWNT), have obtained wide applications in electrochemical detection owing to distinctive properties (*15*−*19*). However, electrochemical oxidation and detection of amaranth using a carbon nanotube-modified electrode is still missing. Herein, a MWNT film-modified glassy carbon electrode (denoted as MWNT/GCE) was successfully used to construct an electrochemical sensor for amaranth. At the MWNT/GCE, an irreversible and greatly improved oxidation peak is observed, suggesting that MWNT film possesses a notable enhancement effect on the oxidation of amaranth. The detection conditions were optimized, and a new electrochemical method was developed for the detection of amaranth. The limit of detection of this sensor is 35 nM, and the analysis time is shorter than 3 min. In addition, this method is more convenient since it is based on the oxidation signal, and the influence of oxygen is negligible.

MATERIALS AND METHODS

Reagents. All the chemicals were of analytical grade and used as received. Amaranth (Sigma) was dissolved into redistilled water to prepare 0.01 M standard solution. The solution was stored in a refrigerator at 4 °C. MWNT (purity >95%) was purchased from Shenzhen Nanotech Port Co. Ltd., China. Dihexadecyl hydrogen phosphate (DHP) was obtained from Sigma.

Instruments. Electrochemical measurements were conducted on an EC 550 Electrochemical Workstation (Gaoss Union Co. Ltd., China) with a conventional three-electrode system. The working electrode is a MWNT/GCE, the reference electrode is a saturated calomel electrode (SCE), and the counter electrode is a platinum wire. Scanning electron microscopy

*Corresponding author. Tel: +86-27-8754 3032. Fax: +86-27-8754 3632. E-mail: kbwu@mail.hust.edu.cn.

 Published on Web 11/09/2010

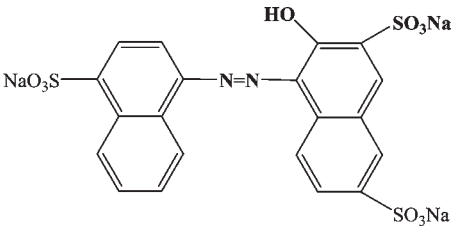

Figure 1. Molecular structure of amaranth.

(SEM) was performed with a Quanta 200 microscope (FEI Company, Netherlands). High performance liquid chromatographic detection was carried out with an Agilent 1100, coupled with a UV−vis detector.

Preparation of MWNT Sensor. In order to disperse MWNT into water easily and homogeneously, DHP was employed due to its easy dispersion in water and strong hydrophobic interaction with MWNT. Ultrasonication of 40 min was used to disperse 10 mg of MWNT and 10 mg of DHP into 10 mL of redistilled water, giving a stable and homogeneous suspension (1 mg mL^{-1}). Before the surface modification, the GCE was polished with 0.05 μm alumina slurry, and then sonicated in redistilled water for 2 min. After that, the GCE surface was coated with 4 μL of MWNT suspension, and the water was evaporated from the surface under an infrared lamp in air. The DHP film-modified GCE (DHP/GCE) was prepared by the same procedure but without MWNT.

Analytical Procedure. Unless otherwise stated, pH 5 acetate buffer (0.1 M) was used as the supporting electrolyte for the detection of amaranth. After 2 min accumulation at 0.2 V, the differential pulse voltammograms were recorded from 0.2 to 1 V, and the oxidation peak current at 0.74 V was estimated. The pulse amplitude is 50 mV, the pulse width is 40 ms, and the scan rate is 40 mV s^{-1}.

Sample Detection. Different soft drinks were purchased from a local market and used directly without any pretreatment. When detecting amaranth using a MWNT sensor, a 0.2 mL sample solution was added into 10.0 mL of pH 5 acetate buffer, and then analyzed according to the analytical procedure. In addition, HPLC was also used to detect amaranth in drinks, and the conditions are as follows. The column was a C18 analytical column (4.6 mm × 150 mm × 5 μm). The gradient mobile phase was methanol (A) and 0.02 M ammonium acetate (B), filtered through a 0.45 μm Millipore filter prior to use. The column was initially equilibrated at 80% mobile phase B. After injection, the concentration of mobile phase B was reduced to 77% over 5 min, and then further decreased to 65% in 7 min and finally to 20% in 12 min. After 12 min, the system was returned to original conditions (mobile phase B at 80%) and equilibrated for 5 min before the next injection. The flow rate was 1 mL min^{-1}, and the sample injection volume was 20 μL. The detection was performed at a wavelength of 230 nm.

RESULTS AND DISCUSSION

Surface Property of MWNT Film. Figure 2 shows the surface morphology of MWNT/GCE, which was characterized using SEM. It is clearly found that the GCE surface was coated with uniform and pure MWNT, and the average diameter is about 40 nm. Moreover, the electrochemical response of 5 mM $K_3[Fe(CN)_6]$ in 1 M KCl at GCE and MWNT/GCE was examined to evaluate their electrochemical active area (not shown). A pair of redox peaks is observed during the cyclic sweep from 0.6 to 0 V, and the peak current increases linearly with the square root of scan rate, indicating a diffusion-controlled process. From the comparison, it is found that the peak current obviously increases at the MWNT film surface. According to the Randles-Sevčik equation, the active area of GCE and MWNT/GCE was calculated to be 0.055 and 0.067 cm^2, suggesting that the MWNT enhances the response area.

Electrochemical Response of Amaranth. The electrochemical behavior of amaranth at different electrodes was studied using cyclic voltammetry (CV), which is shown in **Figure 3**. In pH 5 acetate buffer, just an oxidation peak at 0.89 V is observed at the

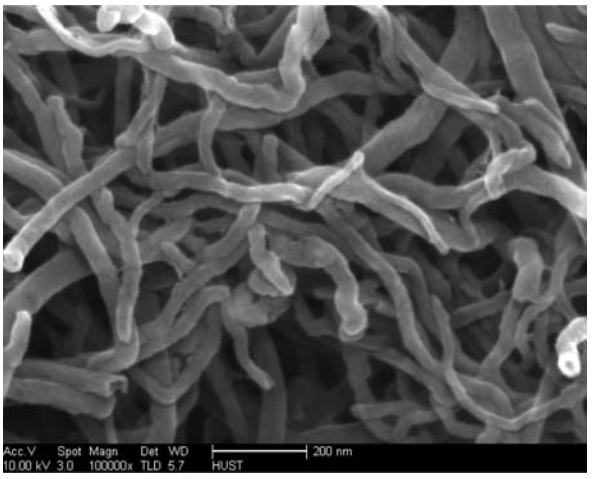

Figure 2. SEM image of MWNT film on GCE surface.

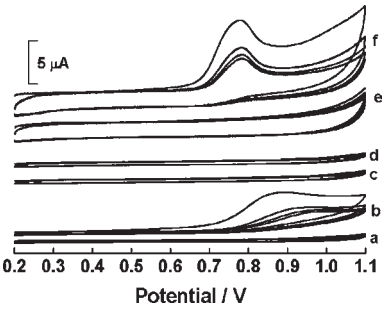

Figure 3. CV curves of 0.1 mM amaranth at GCE (curve b), DHP/GCE (curve d) and MWNT/GCE (curve f) in pH 5 acetate buffer. Curves a, c and e: background of GCE, DHP/GCE and MWNT/GCE. Scan rate = 100 mV s^{-1}.

unmodified GCE for 0.1 mM amaranth (curve b). No reduction peak appears on the reverse scan, indicating the irreversible oxidation of amaranth. When using the DHP/GCE, the oxidation peak vanishes (curve d). This is because DHP, a surfactant with poor electric conductivity, forms a perfect film on the GCE surface and retards the electron transfer of amaranth. However, a greatly improved oxidation peak is observed for amaranth at MWNT/GCE (curve f). Compared with those at the bare GCE, the oxidation peak shifts negatively from 0.89 to 0.78 V, and the peak current obviously increases. The negative shift of oxidation potential and the enhancement of peak current clearly suggest that the MWNT film exhibits highly efficient catalytic activity to the oxidation of amaranth (*20*). In addition, it is also found that the oxidation peak of amaranth remarkably decreases in the second anodic sweep. This is probably due to the adsorption of oxidative products at the electrode surface. As controlled experiments, curves a, c and e depict the voltammetric responses on the GCE, DHP/GCE and MWNT/GCE in pH 5 acetate buffer. They are featureless. Thus, the oxidation peaks in **Figure 3** are caused by the oxidation of amaranth.

The oxidation response of a low concentration of amaranth was then examined using differential pulse voltammetry (DPV). **Figure 4** shows the DPV curves of 0.6 μM amaranth in pH 5 acetate buffer. After 2 min accumulation, a poor-shaped oxidation peak is observed at the unmodified GCE (curve b). The peak potential is 0.79 V, and the peak current is very small, suggesting that the oxidation activity of amaranth is very poor at the GCE surface. However, a very sensitive and well-shaped oxidation peak appears at the MWNT/GCE (curve d). The peak potential is 0.74 V, and the peak current significantly increases, revealing that

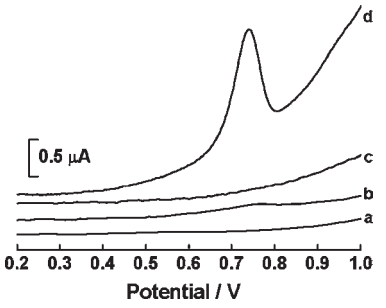

Figure 4. DPV curves of 0.6 μM amaranth at GCE (curve b) and MWNT/GCE (curve d) in pH 5 acetate buffer. Curves a and c: blank curves of GCE and MWNT/GCE. Accumulation time: 2 min. Pulse amplitude: 50 mV. Pulse width: 40 ms. Scan rate: 40 mV s^{-1}.

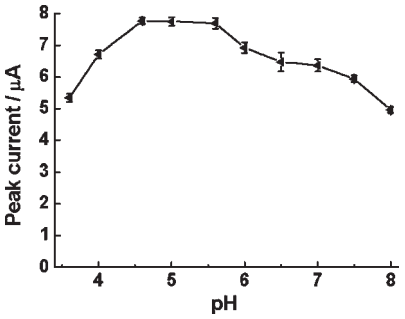

Figure 5. Effect of pH value on the oxidation peak current of 0.1 mM amaranth. The error bars represent the standard deviation of repetitive measurements (n = 3). Other conditions are the same as in **Figure 3**.

the MWNT film exhibits considerable enhancement effect to amaranth. It is well established that MWNT possesses high catalytic activity and electrochemical activity due to edge plane like sites/defects (*21*) or metallic impurities (*22*−*24*). Therefore, the oxidation current signal and the detection sensitivity of amaranth are greatly improved at the MWNT sensor, owing to the high catalytic activity and the strong accumulation efficiency of MWNT film. As shown in curves a and c, the DPV curves for the bare GCE and MWNT/GCE are featureless in the buffer.

Effect of pH Value. The oxidation signal of amaranth at MWNT sensor was examined in different supporting electrolytes to evaluate the influence of pH value. The used solutions include (1) 0.1 M acetate buffer solutions with pH of 3.6, 4, 4.6, 5 and 5.6 and (2) 0.1 M phosphate buffer solutions with pH of 6, 6.5, 7, 7.5, and 8. **Figure 5** depicts the relationship between pH value and the oxidation peak current of 0.1 mM amaranth that obtained from the CV curves. The oxidation peak current of amaranth greatly increases with pH value from 3.6 to 4.6, and then changes very slightly over the pH range from 4.6 to 5.6. When we still increase the pH value up to 8, the oxidation peak current gradually decreases. Herein, the pH 5 acetate buffer was employed to achieve a high and stable response signal.

Influence of Amount of MWNT Suspension. Figure 6 displays the effect of amount of MWNT suspension on the oxidation peak current of amaranth. The oxidation peak current of amaranth increases linearly with the volume of MWNT suspension from 0 to 4 μL. This indicates that MWNT increase the active area of GCE surface, leading to higher accumulation efficiency and larger peak current. When we increase the volume of MWNT suspension up to 8 μL, gradual decline of peak current was noticed, maybe due to the blocking effect of DHP. In order to shorten the time of solvent evaporation and to achieve high sensitivity, 4 μL of MWNT suspension was used to modify the GCE surface.

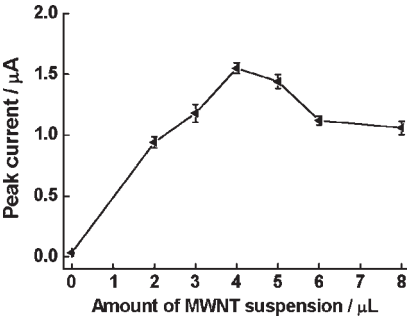

Figure 6. Influence of amount of MWNT suspension on the oxidation peak current of 0.6 μM amaranth. The error bars represent the standard deviation of repetitive measurements (n = 3). Other conditions are the same as in **Figure 4**.

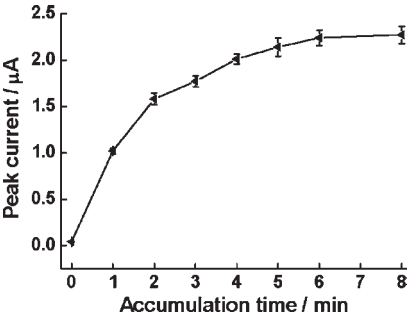

Figure 7. Effect of accumulation time on the oxidation peak current of 0.6 μM amaranth. The error bars represent the standard deviation of repetitive measurements (n = 3). Other conditions are the same as in **Figure 4**.

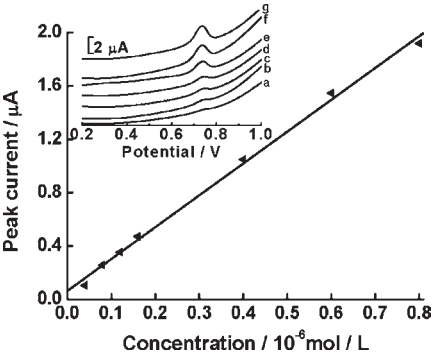

Figure 8. Calibration curve for amaranth. Inset plot: DPV curves of 0.04 (a), 0.08 (b), 0.12 (c), 0.16 (d), 0.4 (e), 0.6 (f) and 0.8 μM (g) amaranth at MWNT/GCE. Other conditions are the same as in **Figure 4**.

Effect of Accumulation Potential and Time. The oxidation peak current of amaranth under open circuit and different accumulation potentials such as −0.2 V, −0.1 V, 0 V, 0.1 V, 0.2 and 0.3 V was individually measured to study the influence of accumulation potential. The oxidation peak current of amaranth keeps constant, revealing no influence of accumulation potential on the detection of amaranth. Therefore, the initial potential (0.2 V in this work) was applied during the accumulation step.

However, the accumulation time has a pronounced effect on the detection of amaranth at the MWNT sensor. As shown in **Figure 7**, the oxidation peak current of amaranth remarkably increases with accumulation time from 0 to 2 min. The adsorption behavior at the MWNT film surface might come from its polymerization at highly positive potential (*25*). When we extend the accumulation time from 2 to 6 min, the degree of peak current

Table 1. Detection of Amaranth in Soft Drinks

no.	by HPLC[a] (mg L^{-1})	by this sensor[a] (mg L^{-1})	rel error	RSD (%)	added (mg L^{-1})	found[a] (mg L^{-1})	recovery (%)
1	13.32	13.54	1.65%	3.9	18.13	19.16	105.7
2	13.47	13.41	−0.45%	3.8	18.13	18.24	100.6
3	13.57	13.39	−1.33%	2.2	18.00	17.25	95.8
4	13.74	13.18	−4.08%	2.1	18.00	18.37	102.1
5	14.13	14.34	1.49%	3.6	18.00	19.36	107.6
6	14.34	14.16	−1.26%	2.4	18.00	16.78	93.2

[a] Values reported are mean of three replicates.

enhancement gradually decreases. Longer accumulation time than 6 min does not enhance the oxidation peak current. Considering sensitivity and working efficiency, 2 min accumulation was used.

Reproducibility. The repeatability for successive measurements using one MWNT sensor was examined. The used sensor was reactivated by three continuous DPV sweeps from 0.2 to 1 V in the supporting electrolyte after each measurement, and then employed for the repeated detection of 0.6 μM amaranth. The relative standard deviation (RSD) is 8.3% for 10 successive measurements. Otherwise, the reproducibility between multiple MWNT sensors was also evaluated by determining in parallel the oxidation peak current of 0.6 μM amaranth. The value of RSD is 5.1% for 11 MWNT sensors. The results indicate that this method possesses good precision for the detection of amaranth.

Linear Range and Limit of Detection. Under optimized conditions, the linear range and limit of detection (LOD) were studied using DPV. As shown in **Figure 8**, the oxidation peak current of amaranth at the MWNT sensor (i_p, μA) is linear to its concentration (C, M) over the range from 40 nM to 0.8 μM. The linear regression equation is $i_p = 0.0625 + 2.389 \times 10^6 C$ ($R = 0.998$). In addition, the LOD was evaluated to be 35 nM (or 21.16 μg L^{-1}) according to IUPAC regulations (S/N = 3).

Interference. The potential interferences for the determination of amaranth were studied. Under the optimized conditions, the oxidation peak current of amaranth was individually measured in the presence of different concentrations of interferents, and the change of peak current was then checked. No influence on the detection of 0.6 μM amaranth was found after the addition of 1000-fold concentrations of glucose, sucrose and glycine; 100-fold concentrations of citric acid, vitamin C, Fe^{3+}, Fe^{2+} and Ca^{2+}; or 20-fold concentrations of tartrazine (the peak current change is below 5%).

Detection of Amaranth in Soft Drinks. In order to test the performance of this method in real sample analysis, it was used to detect amaranth in various soft drinks. Each sample solution undergoes three parallel detections, and the RSD is below 4%, suggesting that the results obtained by the MWNT sensor are acceptable. The content of amaranth was determined by the standard addition method, and the results are listed in **Table 1**. In order to test the accuracy of this method, the content of amaranth was also analyzed by HPLC. The results obtained by HPLC and the MWNT sensor are in good agreement, revealing that this method is satisfactory. In addition, a known amount of amaranth standard was spiked in the sample, and then analyzed according to the same procedure. The value of recovery is in the range from 93.2% to 107.6%, also indicating that this method is accurate and feasible.

ACKNOWLEDGMENT

The Center of Analysis and Testing of Huazhong University of Science and Technology is thanked for its help in the SEM observation.

LITERATURE CITED

(1) Mekkawy, H. A.; Ali, M. O.; El-Zawahry, A. M. Toxic effect of synthetic and natural food dyes on renal and hepatic functions in rats. *Toxicol. Lett*. **1998**, *95*, 155−155.

(2) Tanaka, T. Reproductive and neurobehavioural toxicity study of Ponceau 4R administered to mice in the diet. *Food Chem. Toxicol*. **2006**, *44*, 1651−1658.

(3) Mpountoukas, P.; Pantazaki, A.; Kostareli, E.; Christodoulou, P.; Kareli, D.; Poliliou, S.; Mourelatos, C.; Lambropoulou, V.; Lialiaris, T. Cytogenetic evaluation and DNA interaction studies of the food colorants amaranth, erythrosine and tartrazine. *Food Chem. Toxicol*. **2003**, *48*, 2934−2944.

(4) Llamas, N. E.; Garrido, M.; Di Nezio, M. S.; Band, B. S. F. Second order advantage in the determination of amaranth, sunset yellow FCF and tartrazine by UV-vis and multivariate curve resolution-alternating least squares. *Anal. Chim. Acta* **2009**, *655*, 38−42.

(5) Minioti, K. S.; Sakellariou, C. F.; Thomaidis, N. S. Determination of 13 synthetic food colorants in water-soluble foods by reversed-phase high-performance liquid chromatography coupled with diode-array detector. *Anal. Chim. Acta* **2007**, *583*, 103−110.

(6) Kucharska, M.; Grabkab, J. A review of chromatographic methods for determination of synthetic food dyes. *Talanta* **2010**, *80*, 1045−1051.

(7) Hattori, S.; Doi, M.; Takahashi, E.; Kurosu, T.; Nara, M.; Nakamatsu, S.; Nishiki, Y.; Furuta, T.; Iida, M. Electrolytic decomposition of amaranth dyestuff using diamond electrodes. *J. Appl. Electrochem*. **2003**, *33*, 85−91.

(8) Sun, W.; Jiao, K.; Wang, X. L.; Lu, L. D. Electrochemical studies of the reaction between albumin and amaranth and its analytical application. *J. Electroanal. Chem*. **2005**, *578*, 37−43.

(9) Fan, L.; Zhou, Y. W.; Yang, W. S.; Chen, G. H.; Yang, F. L. Electrochemical degradation of Amaranth aqueous solution on ACF. *J. Hazard. Mater*. **2006**, *137*, 1182−1188.

(10) Fan, L.; Zhou, Y. W.; Yang, W. S.; Chen, G. H.; Yang, F. L. Electrochemical degradation of aqueous solution of Amaranth azo dye on ACF under potentiostatic model. *Dyes Pigment*. **2008**, *76*, 440−446.

(11) Char, M. P.; Niranjana, E.; Swamy, B. E. K.; Sherigara, B. S.; Pai, K. V. Electrochemical studies of amaranth at surfactant modified carbon paste electrode: A cyclic voltammetry. *Int. J. Electrochem. Sci*. **2008**, *3*, 588−596.

(12) Jain, R.; Sharma, N.; Radhapyari, K. Electrochemical treatment of pharmaceutical azo dye amaranth from waste water. *J. Appl. Electrochem*. **2009**, *39*, 577−582.

(13) Ni, Y. N.; Bai, J. L. Simultaneous determination of Amaranth and Sunset Yellow by ratio derivative voltammetry. *Talanta* **1997**, *44*, 105−109.

(14) Alghamdi, A. H. A square-wave adsorptive stripping voltammetric method for the determination of Amaranth, a food additive dye. *J. AOAC Int*. **2005**, *88*, 788−793.

(15) Yang, J. Q.; Wang, P.; Zhang, X. J.; Wu, K. B. Electrochemical sensor for rapid detection of Triclosan using a multiwall carbon nanotube film. *J. Agric. Food Chem*. **2009**, *57*, 9403−9407.

(16) Wan, Q. J.; Wang, X. W.; Yu, F.; Wang, X. X.; Yang, N. J. Poly(taurine)/MWNT-modified glassy carbon electrodes for the detection of acetaminophen. *J. Appl. Electrochem*. **2009**, *39*, 785−790.

(17) Pham, X. H.; Bui, M. P. N.; Li, C. A.; Han, K. N.; Kim, J. H.; Won, H.; Seong, G. H. Electrochemical characterization of a single-walled

carbon nanotube electrode for detection of glucose. *Anal. Chim. Acta* **2010**, *671*, 36−40.
(18) Zhang, Y.; Zhang, X. J.; Lu, X. H.; Yang, J. Q.; Wu, K. B. Multi-wall carbon nanotube film-based electrochemical sensor for rapid detection of Ponceau 4R and Allura Red. *Food Chem*. **2010**, *122*, 909−913.
(19) Hernandez, R.; Riu, J.; Rius, F. X. Determination of calcium ion in sap using carbon nanotube-based ion-selective electrodes. *Analyst* **2010**, *135*, 1979−1985.
(20) Musameh, M.; Wang, J.; Merkoci, A.; Lin, Y. Low-potential stable NADH detection at carbon-nanotube-modified glassy carbon electrodes. *Electrochem. Commun*. **2002**, *4*, 743−746.
(21) Banks, C. E.; Davies, T. J.; Wildgoose, G. G.; Compton, R. G. Electrocatalysis at graphite and carbon nanotube modified electrodes: edge-plane sites and tube ends are the reactive sites. *Chem. Commun*. **2005**, *7*, 829−841.
(22) Sljukic, B.; Banks, C. E.; Compton, R. G. Iron oxide particles are the active sites for hydrogen peroxide sensing at multiwalled carbon nanotube modified electrodes. *Nano Lett*. **2006**, *6*, 1556−1558.
(23) Kruusma, J.; Mould, N.; Jurkschat, K.; Crossley, A.; Banks, C. E. Single walled carbon nanotubes contain residual iron oxide impurities which can dominate their electrochemical activity. *Electrochem. Commun*. **2007**, *9*, 2330−2333.
(24) Merisalu, M.; Kruusma, J.; Banks, C. E. Metallic impurity free carbon nanotube paste electrodes. *Electrochem. Commun*. **2010**, *12*, 144−147.
(25) Wan, Q. J.; Wang, X. X.; Wang, X.; Yang, N. J. Poly(malachite green) film: Electrosynthesis, characterization, and sensor application. *Polymer* **2006**, *47*, 7684−7692.

Received for review August 24, 2010. Revised manuscript received October 28, 2010. Accepted October 28, 2010. This work was supported by the Project of General Administration of Quality Supervision, Inspection and Quarantine of China (200910085 and 2006IK152), the National Basic Research Program of China (973 Program, No. 2009CB320300) and the National Natural Science Foundation of China (No. 61071052).